

The primary ore mineralogy of the Alderley Edge deposit, Cheshire

R. A. IXER AND D. J. VAUGHAN

Department of Geological Sciences, University of Aston in Birmingham, Gosta Green, Birmingham B4 7ET

ABSTRACT. The Alderley Edge deposit, Cheshire, England has been mined principally for Cu and Pb. Here, veins and disseminations occur in coarse-grained clastic sediments of Triassic age and are classified as belonging to the red-bed type of mineralization.

Examination of material in polished and thin section has shown the mineralization to be multiphase. The earliest opaque phases are associated with the diagenesis of the sandstones and include authigenic anatase, plus bravoite, pyrite, and chalcopyrite within authigenic quartz overgrowths. This stage of mineralization was followed by the formation of intergrown bravoite, pyrite, chalcopyrite, sphalerite, and galena accompanied by minor amounts of Ni-Co-Fe sulpharsenides, marcasite, and tetrahedrite cementing the clastic grains. This primary assemblage has undergone extensive alteration resulting in the formation of djurleite, covellite, and blaubleibender covellite accompanied by Pb and Zn carbonates and sulphates. Later, extensive shattering of the cemented clastic grains has been infilled by supergene Cu, Pb, and Zn carbonates and sulphates, limonite, and other secondary minerals.

Electron probe microanalysis of the sulphides shows the pyrite to contain significant Ni and Cu but lesser amounts of Co; the sphalerite to be an Fe-poor variety but to contain Cd, and the chalcopyrite to contain Sb. Ag is present in appreciable amounts in tetrahedrite and occurs in trace amounts in both sphalerite and chalcopyrite but not in galena. The concentration of Ag increases with the alteration of the primary sulphides to secondary sulphides. This is most clearly demonstrated by the alteration of chalcopyrite to an idaite-like phase and finally to djurleite when the Ag content increases from 0.10 to 2.35 wt. %.

THE Permo-Trias rocks of the Cheshire Basin in central England contain a number of small deposits of red-bed type mineralization (Dewey and Eastwood, 1925). The mineralization at Alderley Edge is the most notable and best documented of these, and also still has surface and underground exposures. The mineralization was exploited intermittently from the late 17th century until the early 20th century and produced significant tonnages of Cu and minor amounts of Pb and Co ores, and residues rich in Mn, Ni, Co, and V. A comprehen-

sive account of the mines and mining is given in Carlon (1979).

Alderley Edge is a prominent feature rising approximately 200 m OD in the NE part of the Cheshire Basin about 20 km south of Manchester. It comprises a 3 km wide horst of Triassic rocks bounded by major N.-S. trending faults. Within the horst 250 m of Keuper sediments, mainly conglomerates, sandstones, and mudstones, overlie at least 300 m of Bunter Sandstone. Both the Keuper and Bunter sediments are mainly fluvial in origin although some minor aeolian deposits are also present. Although the stratigraphy has been revised (see Warrington, 1980; Warrington *et al.*, 1980) the older nomenclature is adopted here for simplicity and compatibility with previous mineralogical literature. A number of N.-W. normal faults with small throws of a few metres cross-cut the sediments. Several of these faults contain sulphide and baryte mineralization and the adjacent sandstones are bleached.

The mineralization, which is of Cu, Pb, and Zn plus minor amounts of Ag, Co, V, Ni, and Mn, is found within the top 6 m of the Bunter Sandstone and mainly within three conglomerate and sandstone units of the Keuper Sandstone.

The ores occur as disseminations in the pore-space of the sandstone, or as coarser-grained crystals within fault-breccias. Pb and Zn minerals are especially concentrated close to the small faults whereas the copper mineralization is more widespread and less clearly associated with faulting (Warrington, 1980).

Previous research

General descriptions of the geology of Alderley Edge and its mineralization are given by Dewey and Eastwood (1925), Taylor *et al.* (1963), Mohr (1964), Warrington (1965, 1980), and Carlon (1979). Many of these workers have contributed to the long-standing debate regarding the origin and nature of the mineralization. Most workers have

suggested that the mineralization is epigenetic and related to the faulting and their evidence is summarized by Warrington (1965); but others have suggested that the intimate relationship of the mineralization and its host clastics indicates a wholly or partly syngenetic origin (Dewey and Eastwood, 1925). These models are reviewed by King (1968) and Allen (1980).

Although a wide range of Cu, Pb, and Zn minerals associated with the alteration of the primary ores has been reported from Alderley Edge (these are listed in Warrington, 1980 and Carlon, 1979) there is little detailed mineralogical and petrological information available on the primary ores and almost no geochemical data.

Sampling and laboratory techniques

Representative samples of the Pb and Cu mineralization were collected from both vein-infilling and disseminated ores and from the associated unmineralized sandstones. These included *in situ* Pb-rich vein material from Engine Vein plus its mineralized host sediments and loose material from the Stormy Point and Wood mines including more Cu-rich disseminated ores. Both the Engine Vein and Stormy Point materials occur in the lowest mineralized unit (comprising the topmost Bunter and the basal Keuper) in the ore-bearing succession, whereas the material from Wood Mine occurs within a horizon higher in the Keuper Sandstone (Warrington, 1965).

Over fifty polished sections and polished thin sections were investigated by reflected and transmitted light microscopy. Particular phases were

further studied by X-ray powder diffraction using the Debye-Scherrer camera and by electron probe microanalysis using both Cambridge Instruments Microscan V and ARL-SEM-Q equipment. Carefully characterized pure synthetic sulphides were used as standards and the results subjected to standard correction procedures.

As the main purpose of the investigation was to establish the mineralogy, paragenesis, and possible conditions of formation of the sulphide assemblages, no attempt was made to identify in detail the numerous secondary carbonate, sulphate, and phosphate phases.

Results

The opaque minerals can be divided into four main paragenetic assemblages as shown in fig. 1. The earliest consists of the derived detrital minerals, mainly oxides, and is similar to assemblages found in other sandstones (Ixer *et al.*, 1979). Then an early authigenic assemblage is found with TiO₂ minerals, Fe-Ni sulphides, and chalcopyrite. The succeeding, main mineralization is represented by a primary sulphide cement between the clastic sand grains in the sediments and by the vein-infilling ore. A Cu-rich sulphide cement which replaces the earlier sulphides or, together with carbonates and sulphates, fills voids in the sediments, represents a later alteration of the primary ore.

First assemblage. The detrital assemblage is seen in the altered igneous, metamorphic, or cherty rock fragments and is dominated by the presence of rutile and anatase with lesser amounts of hematite. TiO₂ grains occur as discrete prismatic to rounded

	Detrital Minerals	Inclusions in Quartz Overgrowths	Main Sulphide Cement	Secondary Sulphides
ANATASE, RUTILE	—			
HEMATITE	—	—		
PYRITE	—	—	—	
BRAVOITE		—	—	
Ni-Co-Fe SULPHARSENIDES			—	
MARCASITE			—	
CHALCOPYRITE		—	—	
TETRAHEDRITE			—	
SPHALERITE			—	
GALENA			—	
"IDAITE"				—
DJURLEITE				—
COVELLINE				—

FIG. 1. Paragenetic diagram for the mineralization at Alderley Edge.

twinned rutile grains 6–10 μm in length, or with hematite as pseudomorphs after original Fe–Ti oxide minerals including ilmenite. Hematite occurs as martite pseudomorphs after magnetite or as mosaics or boxwork intergrowths 5–20 μm in diameter. Minor amounts of relict magnetite, ilmenite, and rare chromite (all 10–20 μm in diameter), along with laths of graphite and abundant rounded and zoned zircons, are also part of the detrital fraction. Identical assemblages were found in both the barren and the mineralized sediments.

Second assemblage. Authigenic TiO_2 is common as overgrowths on detrital grains of rutile and anatase but is more abundant as small euhedral ‘octahedrite’ anatase crystals that fill pore spaces. Hematite overgrowths on detrital hematite were not seen. However, the accompanying euhedral quartz overgrowths that enclose many detrital quartz grains also contain fine-grained (1–2 μm) hematite laths together with zoned bravoite, pyrite, and chalcopyrite grains (5–15 μm in diameter). These grains are arranged parallel with the authigenic quartz growth-zones and are totally enclosed within the overgrowths. Hence they are interpreted as being a product of the diagenesis of the sandstone. Within some of the reddened chert clasts a similar assemblage is found, that of acicular hematite crystals, euhedral anatase, poorly crystalline pyrite or pyrite cubes overgrowing framboidal pyrite, euhedral bravoite, and chalcopyrite.

Third assemblage. Sulphides form the main cement between the clastic grains in much of the material that was studied. The clastic grains, particularly the quartz and feldspar, have euhedral quartz and feldspar overgrowths and it is these that are cemented, indicating that the sulphide cement is later than the authigenic production of the quartz and feldspar. In the material from Engine Vein and Stormy Point, galena is the most abundant sulphide, often complexly intergrown with sphalerite and chalcopyrite, with lesser amounts of bravoite and pyrite and trace amounts of marcasite, Ni–Co–Fe sulpharsenides, and tetrahedrite. In the material from Wood Mine and some from Stormy Point Mine, chalcopyrite accompanied by bravoite, pyrite, and galena form the cement. The vein material from Engine Vein comprises galena accompanied by minor quantities of chalcopyrite and sphalerite, and traces of bravoite, pyrite, and tetrahedrite. A consistent paragenesis found in the mineralized sediments is of early bravoite and Ni–Co–Fe sulpharsenides followed by pyrite, chalcopyrite, sphalerite, and finally, galena.

Fourth assemblage. Much of this primary sulphide cement is now replaced by secondary copper

sulphides together with carbonates and sulphates that still retain abundant small (5–10 μm diameter) relicts of the primary phases.

Many of the mineralized sediments show an extensive phase of shattering in which the brittle quartz grains have been extensively fractured; these fractures are infilled with malachite, azurite, and other carbonates and sulphates but carry no sulphides. Limonite occurs in the very oxidized specimens and replaces all phases. Locally it is associated with very fine hematite dust.

Primary minerals

Bravoite. Bravoite forms large (40–80 μm diameter) discrete single crystals or small groups of crystals enclosed in later sulphides. Lilac or brown pentagonal dodecahedra occur and these display multiple colour zoning parallel to the crystal edges. Bravoite is enclosed within pyrite, marcasite, and sphalerite and enclosed and replaced by chalcopyrite and galena. A later, minor, generation of bravoite forms small (5–10 μm wide) veinlets surrounding sphalerite. Subsequent alteration of bravoite is to zoned limonite or secondary copper sulphides.

Nickel–cobalt–iron phases. A number of other Ni–Co–Fe phases occur in trace amounts, some enclosed in bravoite but more often associated with bravoite and pyrite. Their small grain-size (5–10 μm) and complex zoning and intergrowths prevent quantitative identification. Semiquantitative microprobe analyses show the presence of at least three phases. A nickel diarsenide with approximately 5 wt. % Co and showing the optical properties of pararammelsbergite, is enclosed within an Fe-poor Ni–Co sulpharsenide (approximately 16 wt. % Ni, 17 wt. % Co, 0.5 wt. % Fe) that is similar in composition to nickeliferous cobaltite. Optically zoned gersdorffite with variable contents of nickel (\sim 12–16 wt. %), cobalt (\sim 8–11.5 wt. %), and iron (\approx 11–14 wt. %) enclose bravoite.

Pyrite. Pyrite cubes up to 100 μm in diameter are associated with bravoite, chalcopyrite, and minor amounts of marcasite. The marcasite forms rims up to 10 μm in width around pyrite. Pyrite displays colour and hardness zoning typically with a yellow-brown core and white, higher reflectance margins. Electron probe analyses of the pyrite (Table I) show it to contain significant Ni (up to 3.30 wt. %) and Cu (up to 3.20 wt. %) but low Co (up to 0.13 wt. %). Pyrite commonly encloses bravoite, but is itself enclosed in galena and sphalerite and replaced by chalcopyrite. A later and minor generation of pink-brown colloform pyrite is seen as veinlets (5–10 μm in width) surrounding galena. Pyrite is altered to limonite and copper sulphides.

Table 1. Microprobe Analyses of Sulphides from Alderley Edge

Mineral Species	Cu	Fe	Pb	Zn	Cd	Ag	Co	Ni	Mn	Sb	As	S	Total	Remarks
1 Pyrite AE8	2.87	39.99	0.34	0.20	n.d.	0.09	0.13	3.30	n.d.	0.09	0.12	51.29	98.42	Pyrite crystals in main chalcopyrite cement
2 Pyrite AE8	3.20	40.07	0.41	0.11	n.d.	0.09	0.11	2.37	n.d.	n.d.	0.02	51.30	97.68	
3 Chalcopyrite AE32	34.17	29.37	0.37	0.01	0.02	0.09	0.05	n.d.	n.d.	0.23	0.06	34.21	98.59	Relict chalcopyrite in djurleite
4 Chalcopyrite AE23A	34.86	31.02	0.30	0.02	n.d.	0.07	0.07	0.04	0.02	0.97	0.32	33.76	101.44	Unaltered chalcopyrite cement
5 Altered Chalcopyrite AE32	35.95	29.68	0.07	0.02	0.01	0.12	0.07	n.d.	n.d.	0.18	0.10	33.63	99.83	Relict altered chalcopyrite in djurleite
6 Altered Chalcopyrite AE32	38.80	26.28	0.21	0.04	n.d.	0.10	0.06	0.02	n.d.	0.24	0.17	32.41	98.33	Altered chalcopyrite in djurleite
7 Altered Chalcopyrite AE32	39.75	26.75	0.27	0.01	n.d.	0.22	0.03	n.d.	0.02	0.22	0.25	32.66	101.18	"
8 'Idaite' AE23A	47.94	21.77	0.20	0.07	n.d.	0.66	0.04	n.d.	n.d.	0.70	0.16	30.81	102.35	'Idaite' rim to chalcopyrite enclosed in djurleite
9 Sphalerite AE/7	0.05	0.05	0.12	65.04	0.76	0.02	0.03	0.03	0.03	0.06	0.04	32.77	98.00	Unaltered sphalerite cement
10 Sphalerite AE/7	0.08	0.06	0.36	64.65	0.60	0.07	0.03	0.01	n.d.	n.d.	n.d.	33.10	98.96	
11 Sphalerite AE1	0.22	0.12	n.d.	64.41	1.93	n.d.	0.02	n.d.	n.d.	n.d.	0.08	32.19	98.97	Unaltered sphalerite cement
12 Sphalerite AE8	0.22	0.17	n.d.	62.71	2.68	0.05	n.d.	0.04	0.01	n.d.	n.d.	31.80	97.68	
13 Sphalerite AE8	0.52	0.13	0.77	62.84	1.35	0.11	n.d.	0.04	0.01	0.36	n.d.	31.90	98.03	Relict 'brown sphalerite' in djurleite
14 'Brown Sphalerite' AE23A	3.00	0.38	0.07	61.58	4.52	n.d.	0.01	0.02	n.d.	n.d.	0.08	32.27	101.85	
15 Altered Sphalerite AE32	68.31	0.07	0.30	5.95	0.67	0.27	0.02	0.01	n.d.	0.01	0.08	22.12	97.81	Relict 'brown sphalerite' in djurleite
16 Galena AE1	0.04	n.d.	85.90	0.09	0.03	n.d.	n.d.	n.d.	0.02	n.d.	n.d.	13.26	99.34	Unaltered galena cement
17 Galena AE7	0.02	0.03	85.78	n.d.	0.02	n.d.	n.d.	0.03	n.d.	0.04	n.d.	13.37	99.29	
18 Galena AE8	0.03	n.d.	87.84	0.08	0.07	n.d.	0.03	0.06	n.d.	0.07	n.d.	13.53	101.51	Djurleite after chalcopyrite
19 Djurleite AE23A	74.54	3.17	n.d.	0.04	n.d.	1.58	n.d.	0.05	n.d.	0.58	0.14	20.94	101.04	
20 Djurleite AE32	75.28	0.92	0.13	0.01	0.08	1.17	0.02	0.04	n.d.	0.74	0.03	21.13	99.55	Djurleite after sphalerite
21 Djurleite AE32	77.06	0.80	n.d.	0.05	0.04	2.35	n.d.	n.d.	n.d.	0.07	0.06	21.47	101.90	
22 Djurleite AE32	76.07	0.84	0.17	0.04	n.d.	1.38	n.d.	0.04	0.01	0.16	0.09	22.43	101.23	Djurleite after 'idaite'
23 Djurleite AE32	74.71	0.26	0.13	0.03	n.d.	0.68	n.d.	0.02	n.d.	0.20	0.05	21.98	98.06	
24 Djurleite AE32	75.75	0.12	n.d.	0.06	0.01	0.46	0.04	n.d.	0.04	0.11	0.04	21.77	98.40	
1. (Fe _{0.90} Mn _{0.07} Cu _{0.06}) ₂ S			9. Zn _{0.97} S											17. Pb _{0.99} S
2. (Fe _{0.90} Ni _{0.05} Cu _{0.06}) ₂ S			10. Zn _{0.96} S											18. Pb _{1.02} S
3. Cu _{1.01} Fe _{0.97} S ₂			11. (Zn _{0.98} Cd _{0.02}) ₂ S											19. (Cu _{1.80} Fe _{0.09} Ag _{0.02}) ₂ S
4. Cu _{1.04} Fe _{1.05} S ₂			12. (Zn _{0.97} Cd _{0.02}) ₂ S											20. (Cu _{1.80} Fe _{0.02} Ag _{0.02}) ₂ S
5. Cu _{1.08} Fe _{1.01} S ₂			13. (Zn _{0.97} Cd _{0.01}) ₂ S											21. (Cu _{1.81} Fe _{0.02} Ag _{0.03}) ₂ S
6. Cu _{1.21} Fe _{0.93} S ₂			14. (Zn _{0.94} Cd _{0.04} Cu _{0.05}) ₂ S											22. (Cu _{1.71} Fe _{0.02} Ag _{0.02}) ₂ S
7. Cu _{1.23} Fe _{0.94} S ₂			15. Cu _{1.56} Zn _{0.13} S											23. (Cu _{1.72} Ag _{0.01}) ₂ S
8. Cu _{3.14} Fe _{1.62} S ₄			16. Pb _{1.00} S											24. Cu _{1.76} S

Chalcopyrite. Anhedronal chalcopyrite (60–80 μm in diameter) is intimately intergrown with sphalerite and galena in the main primary cement. It encloses both bravoite and pyrite but is enclosed in sphalerite, often as euhedral crystals (20–40 μm) surrounded by a thin (2–5 μm) rim of galena. In galena the enclosed chalcopyrite is intergrown with sphalerite and trace amounts of tetrahedrite. Analyses of chalcopyrite (Table I) show it to contain up to 0.09 wt. % Ag and up to 0.97 wt. % Sb but lesser amounts of As (up to 0.32 wt. %). The subsequent alteration of chalcopyrite is extensive and variable and is initiated along fractures, cleavages, and crystal boundaries. It alters to a brown anisotropic mineral with properties close to those of 'idaite', or to bornite, djurleite, covelline, blaubleibender covelline, cuprite, limonite, malachite, and azurite. Although adjacent chalcopyrite crystals can show quite different alteration sequences a generalized sequence of alteration is 'idaite'–bornite succeeded by rims of djurleite–'chalcosine', covelline–blaubleibender covelline, limonite–cuprite, and finally, malachite–azurite. Electron probe analyses of the alteration of chalcopyrite to 'idaite' (Table I) show a progressive increase in Cu from 35.95 to 47.94 wt. % and decrease in Fe from 29.68 to 21.77 wt. %, and an increase in the Ag values with alteration from 0.12 to 0.66 wt. %. No systematic change in either Sb or As values could be established.

Tetrahedrite. Tetrahedrite forms small 5–15 μm green-grey anhedronal crystals intergrown with sphalerite all of which are enclosed in galena. This is especially the case in the vein material from Engine Vein. Semiquantitative microprobe analysis of tetrahedrite in galena showed a high Ag content (~ 14 wt. %) and significant Zn (~ 8 wt. %) with Cu, Sb, and S the only other elements present.

Sphalerite. Sphalerite displays light coloured or, more rarely, dark orange or purple internal reflections. It is intimately intergrown with galena and to a lesser extent with chalcopyrite and pyrite. Against galena it displays euhedral boundaries. It encloses bravoite, pyrite, chalcopyrite, and tetrahedrite but is commonly enclosed in galena. Table I shows typical sphalerite compositions; it is an Fe-poor sphalerite containing up to 0.17 wt. % Fe but it does contain significant Cd (< 2.68 wt. %) and a little Ag (< 0.11 wt. %). Like chalcopyrite, sphalerite displays variable alteration and is commonly totally pseudomorphed by secondary minerals. The alteration sequence is to a darker 'brown' sphalerite that is enriched in Cd (up to 4.52 wt. %), Cu (up to 3.00 wt. %), and Fe (up to 0.38 wt. %), to djurleite, covelline, blaubleibender covelline, smithsonite, and limonite.

Galena. Galena is the main sulphide cement in

most of the material studied. It encloses all the other primary sulphides although it is sometimes veined by thin (2–5 μm wide) veinlets of pyrite–chalcopyrite. Galena contains very rare inclusions (1–2 μm size) of a white native metal and 2 μm long inclusions of a brown-lilac anisotropic mineral. Analyses of the galena (Table I) show it to contain less Ag (below the detection limit of the technique) than the other primary sulphides. Galena is extensively altered to djurleite, covelline, blaubleibender covelline, cerussite, and anglesite.

Secondary minerals

All of the primary sulphides have been extensively altered to secondary Cu sulphides or to carbonates and sulphates. The secondary Cu sulphides themselves form a volumetrically important cement for the sandstones and show a number of distinctive fabrics. These include fine intergrowths of two or more sulphides pseudomorphing earlier minerals and boxworks of acicular sulphides oriented along cleavages of the primary minerals. In addition, the Cu sulphides form void-filling textures in the pore-spaces of the sediments, including botryoidal and rhythmic crustification textures, plumose and rosette structures.

Djurleite. The main secondary Cu sulphide is white to pale blue and anisotropic and has been identified by X-ray diffraction as djurleite. Minor amounts of a blue isotropic Cu sulphide that replaces chalcopyrite are identified as chalcosine. Djurleite forms mosaics of small (~ 5 μ diameter) crystals that replace chalcopyrite, galena, and sphalerite; often the djurleite is complexly intergrown with covelline, blaubleibender covelline, or Cu and Pb carbonates. Djurleite also occurs as rhythmically precipitated crusts of acicular crystals alternating with covelline and Cu carbonates, or as botryoidal crusts alternating with cerussite and smithsonite. Analyses of the djurleite (Table I) show it to contain Ag values (0.46–2.35 wt. %) that are significantly higher than those in earlier sulphides, with the exception of tetrahedrite. Djurleite alters along grain boundaries to covelline and blaubleibender covelline, and then to malachite and azurite.

Covelline. Covelline and blaubleibender covelline occur together replacing all other sulphides. Covelline also forms acicular or plumose crystals collected into small rosettes (20 μm diameter) which are void infillings occurring in association with carbonates and sulphates, and particularly with malachite.

Non-sulphides. X-ray diffraction shows that the most common non-sulphide secondary minerals

are anglesite, cerussite, and smithsonite. Smithsonite replaces sphalerite and typically forms rounded zoned crystals, whilst cerussite and anglesite replace galena, often with 2–3 μm relict galena inclusions. Malachite and azurite form botryoidal masses or fibrous crystals or euhedral rhombic crystals growing into voids.

Discussion of results

Study of the primary ore minerals at Alderley Edge shows that there were several phases of mineralization (fig. 1). The detrital and authigenic oxide component of the opaque mineral association is dominated by TiO_2 minerals and shows a distinct depletion in detrital hematite compared to normal red sediments. This is, however, similar to the associations observed in other *bleached* red sandstones (Ixer *et al.*, 1979). The early authigenic assemblage comprises not only TiO_2 minerals but also minor sulphides containing Fe, Ni, and Cu. It is very minor in terms of the amounts of metals involved but may be of genetic interest. This phase of mineralization was succeeded by the main sulphide mineralization in which the consistent paragenetic sequence of Fe–Ni–Co sulphides and sulpharsenides, followed by Cu–Fe, then Zn, and finally Pb sulphides is observed. Associated with this major phase of mineralization was the introduction of minor amounts of Ag, Cd, and Sb. Sulphides of the main phase were later altered and replaced by Cu sulphides which are so abundant as to suggest that additional Cu may have been introduced at this stage. Processes of oxidation and weathering of the sulphide ores, accompanied by episodes of shattering, have produced an extensive suite of carbonates, sulphates, and associated minerals.

Analysis of the major ore minerals (Table I) has shown pyrite to contain significant Ni and to be remarkably high in Cu content. The sphalerite contains some Cu, is very poor in Fe, and significantly enriched in Cd. Altered varieties of sphalerite show further enrichment in Cu and Cd. The galena analyses are notable for the absence of elements other than Pb and S; in particular, no enrichment in Ag has been observed. Ag is found in substantial amounts in tetrahedrite, although this is a rare mineral at Alderley Edge, and in trace amounts in sphalerite, and in more significant minor concentrations in the chalcopyrite. However, much of the Ag has been concentrated in the secondary Cu sulphide, djurleite, which may hold up to 2.35 wt. % Ag. This effect is well shown in fig. 2, a series of X-ray backscatter pictures obtained from the electron probe microanalyser. Here a grain of chalcopyrite containing trace Ag is surrounded and replaced by djurleite which has much

higher concentrations of Ag. The Ag is almost certainly contained within the djurleite lattice; chalcosine can accommodate a few per cent Ag at low temperatures (Skinner, 1966) and there are similarities in the structural chemistry of Cu and Ag sulphides which suggest such substitution probably also occurs in djurleite.

In some cases the alteration of chalcopyrite to djurleite takes place via an intermediate 'altered chalcopyrite' phase which has optical properties similar to those reported for idaite and nukundamite but which is too small to characterize further other than to provide analyses which show Cu enrichment and Fe depletion (Table I). It is significant that Ag also shows enrichment with the sequence of maximum observed concentrations being chalcopyrite (0.09 wt. %)-'idaite' (< 0.66 wt. %)-djurleite (< 2.35 wt. %).

Conditions of mineralization

Using the relatively simple primary ore mineral assemblages observed at Alderley Edge it is difficult to deduce much regarding the physico-chemical conditions of mineralization. Unfortunately, no data are available from studies of fluid inclusions which might enable temperatures and salinities of the ore-forming fluids to be estimated. It is reasonable to assume that during the main episode of sulphide mineralization, solutions were depositing pyrite, chalcopyrite, and sphalerite with a low iron content (averaging ~ 0.1 mol % FeS). The conditions of sulphur activity as a function of temperature under which such an assemblage would be stable can be estimated from published data (Scott and Barnes, 1971; Vaughan and Craig, 1978) but require further limiting information on either temperature or a_{S} . However, intersection of sulphidation curves for sphalerite containing 0.1 mol % FeS and that defining pyrite–pyrrhotine fields does suggest a very tentative minimum to temperature and sulphur activity values of $\sim 60^\circ\text{C}$ and 10^{-29} atm.

The nature and origin of the mineralizing solutions responsible for the Alderley Edge deposits is conjectural but a number of observations can be made in the light of this study. Emphasis has previously been placed on the high Co:Ni ratio in galenas as indicating a partly magmatic source (Mohr, 1964; Warrington, 1965). The data presented here do not confirm this result and as previously noted (Vaughan and Ixer, 1980) such trace metals reported in bulk analyses of sulphides frequently derive from small inclusions of discrete phases within host galenas. The primary ore mineral assemblages at Alderley Edge show similarities to other 'red-bed' Cu–Pb–Zn deposits (Maubach and Mechernich, Germany; Schachner,

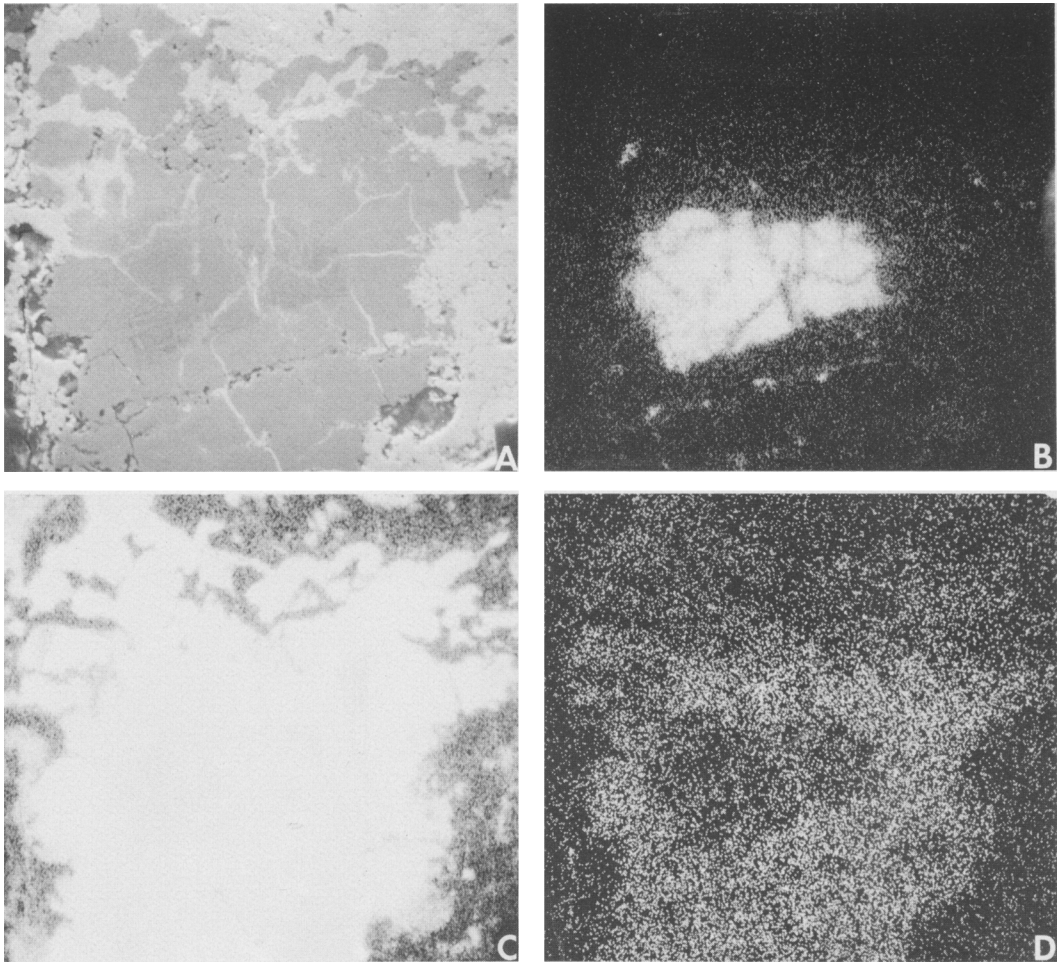


FIG. 2. Electron probe scanning micrographs of chalcopyrite in djurleite: (a) electron backscatter; (b) Fe- $K\alpha$ X-rays; (c) Cu- $K\alpha$; (d) Ag- $L\alpha$.

1961; Largentière, France: Samama, 1976), but also show marked similarities to the mineralization found in the North Pennine Orefields (e.g. the Alston Block Area: Vaughan and Ixer, 1980; Ixer, 1978) which are known from fluid inclusion studies to have been relatively low-temperature brines.

Although the field evidence suggests that much of the mineralization is epigenetic, the textural evidence for some concentration of Fe, Ni, and Cu sulphides during diagenesis of the sandstone suggests that syngenetic processes also have a role in the red-bed mineralization at Alderley Edge. The extent and importance of these syngenetic processes remains to be assessed.

Acknowledgements. Receipt of a contract (No. MPP-155-81-UK(M)) from the Commission of the European Com-

munities Research and Development Programme is gratefully acknowledged. Certain of the electron probe analyses were carried out at the Department of Geological Sciences, Virginia Polytechnic Institute and State University when one of us (DJV) was on a Visiting Professorship. Thanks are due to the Head of Department for the hospitality afforded and also to Todd Solberg who provided help and advice in the use of the instrument. Dr G. Warrington is thanked for his useful criticism of the manuscript.

REFERENCES

- Allen, P. M. (1980) In *European Copper Deposits*. Dept. Econ. Geol. Belgrade. 266-76.
 Carlon, C. (1979) *The Alderley Edge Mines*. John Sherratt and Sons.
 Dewey, H., and Eastwood, T. (1925) *Copper ores of the*

- Midlands, Wales, the Lake District and the Isle of Man.* Mem. Geol. Surv., Spec. Rept. Min. Resources G.B. 30. H.M.S.O.
- Ixer, R. A. (1978) *Mineral. Mag.* **42**, 149-50.
- Turner, P., and Waugh, B. (1979) *Geol. J.* **14**, 179-92.
- King, R. J. (1968) In *Geology of the East Midlands.* Leicester Univ. Press. 112-37.
- Mohr, P. A. (1964) *Contrib. Geophys. Obs. Fac. Sci. Haile Selassie Univ. Ser. A-4.* 1-59.
- Samama, J. C. (1976) In *Handbook of stratabound and stratiform ore-deposits.* Elsevier 6. 1-20.
- Schachner, D. (1961) *Aufschluss. Soderh.* **10**, 43-9.
- Scott, S. D., and Barnes, H. L. (1971) *Econ. Geol.* **66**, 653-69.
- Skinner, B. J. (1966) *Ibid.* **61**, 1-26.
- Taylor, B. J., Price, R. H., Trotter, F. M. (1963) *Geology of the country around Stockport and Knutsford.* Mem. Geol. Surv. H.M.S.O.
- Vaughan, D. J., and Craig, J. R. (1978) *Mineral chemistry of metal sulphides.* Cambridge Univ. Press.
- and Ixer, R. A. (1980) *Trans. Inst. Min. Metall.* **89**, B99-109.
- Warrington, G. (1965) *Mercian Geol.* **1**, 111-29.
- (1980) *Amateur Geol.* **8**, 4-13.
- Audley-Charles, M. G., Elliott, R. E., Evans, W. B., Ivimey-Cook, H. C., Kent, P. E., Robinson, P., Shotton, F. W., and Taylor, F. M. (1980) *A correlation of Triassic rocks in the British Isles.* Geol. Soc. Lond. Spec. Rept. 13. 78 pp.

[Manuscript received 9 October 1981;
revised 25 January 1982]